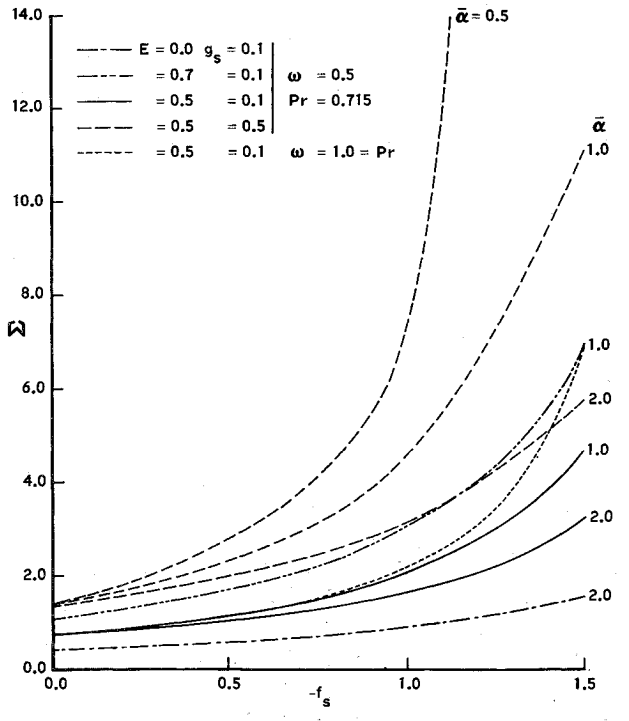

Fig. 2 Influence of injection on the skewing of the flow within the boundary layer.

percent. In Table 6, the influence of the flow energy parameter is displayed to complete the data.

Table 6 Influence of E_1 on $\tau_{1,s}{}^*/\tau_{1,s,0}{}^*$, $\omega = 0.5$, $Pr = 0.715$, $g_s = 0.1$

$\bar{\alpha}$	$E = 0.0$	0.5	0.7	0.9
0.0	1.00	1.00	1.00	1.00
0.5	1.26	1.30	1.34	1.49
1.0	1.48	1.54	1.00	1.77
2.0	1.84	1.92	2.02	2.28
3.0	2.03	2.25	2.36	2.68

We now have sufficient data to estimate accurately the effects of Mach number, wall to total enthalpy ratio and angle of attack on the meridional shear stress and heat transfer to the most windward meridians of cones at angles of attack.

Finally, with the view of evaluating the validity of the small cross-flow assumption, we turn to the purely kinematic aspects of the flow. If we define skewness of the flow Σ as the difference between the tangents of the flow angles across the boundary layer (i.e., $u_{2,s}/u_{1,s} - u_{2,e}/u_{1,e})/(u_{2,e}/u_{1,e})$, then,

$$\Sigma = f_{2,s}''/f_{1,s}'' - 1 \tag{7}$$

Selected data are shown in Fig. 2 to indicate the strong effect of injection on Σ. These results suggest that the small cross-flow assumption should be reexamined in situations involving injection.

This Note demonstrates that normalization of heat-transfer and shear stress data by the zero angle-of-attack values eliminates the influence of gas properties. Further, it is shown that the normalized heat-transfer and meridional shear stress values are almost identical so that the more readily available experimental heat-transfer data may be used to estimate shear stress. A wide range of conditions is considered to provide sufficient data for engineering estimates.

References

[1] Moore, F. K., "Three-Dimensional Compressible Laminar Boundary-Layer Flow," TN 2279, 1951, NACA.

[2] Reshotko, E., "Laminar Boundary Layer with Heat-Transfer on a Cone at Angle of Attack in a Supersonic Stream," TN 4152, 1957, NACA.

[3] Dwyer, H. A., "Boundary Layer on a Hypersonic Sharp Cone at a Small Angle of Attack," *AIAA Journal*, Vol. 9, No. 2, Feb. 1971, pp. 277–284.

[4] Boericke, R. R., "Laminar Boundary Layer on a Cone at Incidence in Supersonic Flow," *AIAA Journal*, Vol. 9, No. 3, March 1971, pp. 462–468.

[5] Fannelop, T. K. and Smith, P. C., "Three-Dimensional Boundary-Layer Flow about an Ablating Slender Cone," ASME Paper 69-FE-23, presented at the Applied Mechanics and Fluids Engineering Division, Evanston, Ill., June 1969.

[6] Libby, P. A., "Three-Dimensional Boundary Layer Flow with Uniform Mass Transfer," *The Physics of Fluids*, Vol. 12, No. 2, Feb. 1969, pp. 408–417.

[7] Chan, Y. Y., "A Note on a Similarity Transformation for Three-Dimensional Compressible Laminar Boundary-Layer Equations," Aeronautics Rept. LR-469, Nov. 1967, National Aeronautical Establishment, Ottawa, Canada.

[8] Cohen, N. B., "Boundary-Layer Similar Solutions and Correlation Equations for Laminar Heat Transfer Distribution in Equilibrium Air at Velocities up to 41,000 Feet per Second," TR-118[illegible]061, NASA.

[9] Wortman, A., "Mass Transfer in Self-Similar Boundary-Layer Flows," Report, Aug. 1969, Northrop Corp., Hawthorne, Calif.; also Ph.D. dissertation, Aug. 1969, Dept. of Engineering and Applied Science, Univ. of California, Los Angeles, Calif.

[10] Wortman, A. and Mills, A. F., "Mass Transfer Effectiveness at Three-Dimensional Stagnation Points," Vol. 9, No. 6, June, 1971, pp. 1210–1212.

[11] Leigh, D. C. and Ross, B. B., "Surface Geometry of Three-Dimensional Inviscid Hypersonic Flow," *AIAA Journal*, Vol. 7, No. 1, Jan. 1969, pp. 123–129.

[12] "Equations, Tables and Charts for Compressible Flow," Rept. 1135, 1953, NACA.

Nonstationary Response Exceedance Statistics of a Simple Mechanical System

JOSEPH M. VERDON*
University of Connecticut, Storrs, Conn.

Introduction

THIS Note concerns the response of a single degree-of-freedom system to a type of nonstationary random excitation. The parameter of particular interest is the expected frequency of exceedances of given levels by the displacement response. The motion of the system is governed by the familiar equation

$$\ddot{x}(t) + 2\zeta\omega_n\dot{x}(t) + \omega_n{}^2 x(t) = \dot{y}(t)/m \tag{1}$$

and the excitation or forcing function is of the form

$$y(t) = n(t)g(t) = n(t)(1+\beta\sin\omega t)[U(t-t_0) - U(t-t_f)] \tag{2}$$

where $n(t)$ is stationary Gaussian noise with zero mean and $U(t)$ denotes the unit step function. It is assumed that the system is stable with less than critical damping ($0 < \zeta < 1$), and that the noise is exponentially correlated, i.e.,

$$E\{n(t_1)n(t_2)\} = R_{nn}(t_2 - t_1) = \sigma_n{}^2 \exp[-\alpha|t_2 - t_1|] \tag{3}$$

The present work has been motivated by a study of the response of aircraft to atmospheric turbulence. The aircraft is usually modeled as a linear system and turbulent forces as

Received August 31, 1971; revision received February 3, 1972. This work was performed during the author's tenure as an ASEE-NASA Summer Faculty Fellow in the Aerodynamic Loads Branch at NASA Langley Research Center, Hampton, Va. The assistance of R. Steiner is gratefully acknowledged.

Index category: Aircraft Gust Loading and Wind Shear.

* Assistant Professor of Mechanical Engineering.

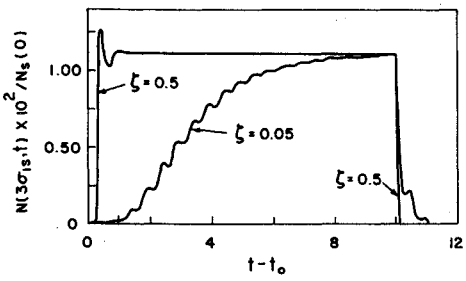

Fig. 1 Normalized expected frequency of displacement exceedances of the level $\gamma = 3\sigma_{1S}$ due to a constant intensity excitation acting for a finite time interval.

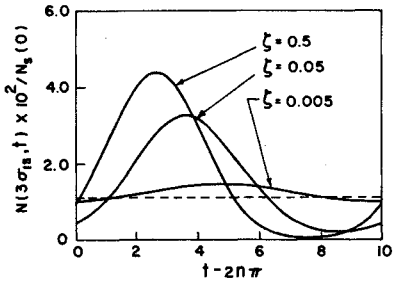

Fig. 3 Normalized expected frequency of the displacement response to variable intensity excitation exceeding the level $\gamma = 3\sigma_{1S}$, $\beta = 0.2$.

stationary and Gaussian random processes. Under these conditions, predictions of the number of response exceedances above a certain level per unit time, $N(\gamma)$, vs the level exceeded γ appear as a straight line on a $\log N(\gamma)$ vs γ^2 plot. Observed data indicates that theoretical predictions for exceedance frequencies are conservative especially at large values of γ[1]. The lack of agreement between observation and theoretical prediction has usually been attributed to the non-Gaussian structure of the turbulence. However, on the basis of a recent analytical and experimental investigation, Piersol[2] has attributed the discrepancy between theory and observed data to nonstationary trends in the variance of such data.

Piersol's conclusion indicates the desirability of further studies of the influence of nonstationary excitation on system response. In the present effort a simple model of the excitation experienced by an aircraft moving through a patch of turbulence of finite length and variable intensity is considered. The objective is to illustrate the effect of these two types of nonstationarity on the displacement exceedance frequencies of a single degree-of-freedom system.

Response Formulation

The expected number of upward crossings of the level γ per unit time by the displacement response is given by Rice's expression

$$N(\gamma, t) = \int_0^\infty \dot{x} f(\gamma, \dot{x}, t)\, d\dot{x} \tag{4}$$

When the input to the system is Gaussian the displacement and velocity are jointly Gaussian, and their joint probability density function, $f(x, \dot{x}, t)$, is completely defined in terms of the mean values of displacement and velocity, the mean square displacement, $X_{11}(t) = E\{x^2(t)\}$, and velocity $X_{22}(t) = E\{\dot{x}^2(t)\}$, and the displacement-velocity correlation, $X_{12}(t) = E\{x(t)\dot{x}(t)\}$. The system is assumed to be at rest for $t \leqq t_0$ and the excitation has zero mean. Hence, the displacement and velocity will have zero mean, and it follows after integration of Eq. (4) that[3]

$$N(\gamma, t) = D^{1/2}\exp(-\gamma^2 X_{22}/2D)/(2\pi X_{11}) + \gamma X_{12}\exp(-\gamma^2/2X_{11})\{1+\operatorname{erf}[\gamma X_{12}/(2X_{11}D)^{1/2}]\}/(8\pi X_{11}{}^3)^{1/2} \tag{5}$$

where $D = X_{11}X_{22} - X_{12}{}^2$ and erf denotes the error function.

The response correlation matrix $X(t) = [X_{ij}(t)]$ is determined from the equation

$$X(t) = \int_{t_0}^{t}\int_{t_0}^{t} \Phi(t, \xi) Y(\xi, \eta) \Phi^*(t, \eta)\, d\xi\, d\eta \tag{6}$$

where Φ and Φ^* are the state transition matrix of the system[4] and its transpose respectively, and Y is the input correlation matrix, i.e.,

$$Y(\xi, \eta) = m^{-2} g(\xi) g(\eta) \begin{bmatrix} 0 & 0 \\ 0 & R_{nn}(\eta - \xi) \end{bmatrix} \tag{7}$$

Values of the response correlations are obtained by integration of Eq. (6) and these in turn are substituted into Eq. (5) to determine $N(\gamma, t)$.

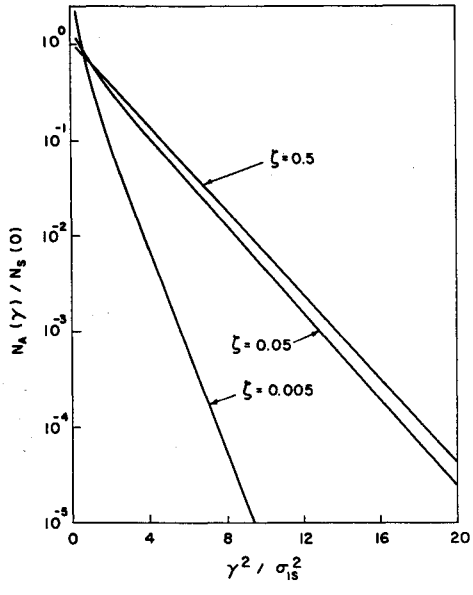

Fig. 2 Normalized time-average expected frequency of displacement exceedances of various levels due to constant intensity excitation acting for a finite time interval.

Results and Discussion

For purposes of illustration it is convenient to treat the two nonstationary aspects of the excitation separately. In the first case the effect of the input acting over a finite time interval is considered, and the excitation intensity is maintained at a constant value ($\beta = 0$). In the second, the effect of a variable intensity input is examined and the response is considered at times large enough so that transient motions have disappeared. A system with $\omega_n = 2\pi$ and input noise with $\alpha = 2\pi$ was considered. For the constant intensity case the input was applied for a time interval equal to ten natural periods of the system and for the variable intensity case the frequency of the modulating function was set equal to one-tenth of the system natural frequency and the response was determined for times $t > 2n\pi$ where n is an integer large enough to insure that transient motions are negligible.

Results for constant intensity excitation applied over a finite time interval appear in Figs. 1 and 2. Figure 1 depicts the temporal behavior of the normalized expected frequency of upward crossings of the level $\gamma = 3\sigma_{1S}$ by the nonstationary displacement response. σ_{1S} and $N_S(0)$ represent the stationary rms displacement and expected frequency of zero crossings, respectively. As the damping ratio increases, the time required for the response exceedance frequency to reach its stationary level decreases and the response decays more rapidly to the rest state after the excitation stops. Curves of the ratio $N_A(\gamma)/N_S(0)$ versus $\gamma^2/\sigma_{1S}{}^2$ appear in Fig. 2. $N_A(\gamma)$ is defined by the relation

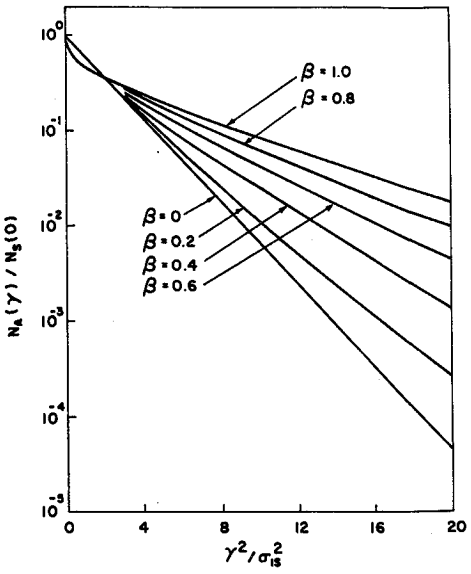

Fig. 4 Normalized time-average expected frequency of the displacement response to variable intensity excitation exceeding various levels, $\zeta = 0.5$.

$$N_A(\gamma) = \int_{t_0}^{\infty} N(\gamma, t)\, dt/(t_f - t_0) \tag{8}$$

For $\gamma^2/\sigma_{1S}{}^2 > 1.5$ this ratio increases with system damping. The curve for $\zeta = 0.5$ practically coincides with stationary values, i.e., $N_S(\gamma)/N_S(0)$, over most of its length. These results indicate that for a lightly damped system, unless the excitation time interval is large, it is necessary to include transient effects to make reliable estimates of exceedance statistics. For the example studied stationary estimates for the expected number of displacement exceedances above high levels are conservative, since the influence of transient motions was to reduce the values of this parameter.

The temporal behavior of the normalized expected frequency of displacement exceedances of the level $\gamma = 3\sigma_{1S}$ for a variable intensity input is illustrated in Fig. 3. The dashed line denotes the stationary value of this parameter. It is readily observed that the number of displacement exceedances above the level $3\sigma_{1S}$ will be greater in the case of the prescribed variable intensity excitation. Curves of the ratio $N_A(\gamma)/N_S(0)$ vs $\gamma^2/\sigma_{1S}{}^2$ for $\zeta = 0.5$ and selected values of β appear in Fig. 4. In this case $N_A(\gamma)$ was obtained by averaging $N(\gamma, t)$ over one period of the modulating function. The average expected frequency of exceeding high levels, $\gamma > 2\sigma_{1S}$, increases as the amplitude of the modulating function increases. This effect is more pronounced at the higher levels and for heavily damped systems. The trends indicated in Fig. 4 are the same as those observed for atmospheric turbulence data,[1,5] i.e., observed values of exceedance frequencies are similar to the $\beta = 0.2$ and $\beta = 0.4$ curves while the theoretical prediction is given by the $\beta = 0$ curve.

References

[1] Dutton, J. A., "Effects of Turbulence on Aeronautical Systems," *Progress in Sciences*, 1st ed., Vol. 11, Pergamon Press, Oxford, England, 1970, pp. 67–109.

[2] Piersol, A. G., "Investigation of the Statistical Properties of Atmospheric Turbulence Data," TR MAC 28032-07, 1969, Measurement Analysis Corp., Marina Del Rey, Calif.

[3] Howell, L. J., "Response of Flight Vehicles to Nonstationary Random Atmospheric Turbulence," Ph.D. thesis, 1971, University of Illinois, Urbana, Ill.

[4] Zadeh, L. A. and Desoer, C. A., *Linear System Theory*, 1st ed., McGraw-Hill, New York, 1963, pp. 294–300.

[5] Atnip, F. K. and Gault, J., "An Analysis of Gust Velocities for Application to Aircraft Design," *International Conference on Atmospheric Turbulence*, Royal Aeronautical Society, London, May, 1971.

Artificial Viscosity Methods for Blunt Body Flowfield Analysis with Thermal Radiation

JAMES O. NICHOLS*
Auburn University, Auburn, Ala.

Nomenclature

e = energy per unit volume
h = computational mesh length
p = pressure
t = time
T = temperature
u_i = velocity in x_i direction
x, y = Cartesian coordinates in direction parallel to and normal to, respectively, the freestream direction
σ = Stefan-Boltzmann constant
σ_0 = constant time-step parameter at initial conditions
ω = constant artificial viscosity parameter

Introduction

ARTIFICIAL viscosity methods have been used to successfully predict flowfields about bodies[1,2] including the effects of angle of attack and nonequilibrium flow. The purpose of this investigation was to determine the effects of including thermal radiation in two of these methods. The two artificial viscosity methods chosen, Lax's[3] and Rusanov's[4] methods, were selected because of their simplicity and because Lax's method assumes a constant artificial viscosity coefficient while Rusanov's method allows the artificial viscosity coefficient to vary with position in the flowfield. A modification to Lax's method is also presented which greatly strengthens the stability of the equations.

The investigation was conducted at two Mach numbers, 10 and 30. The lower was chosen because it represents an approximate lower bound at which thermal radiation may be important and the upper represents the approximate bound for the gray, optically thin gas assumption.

The body chosen for this investigation was a two-dimensional, semi-infinite, planar body with a thickness of 1 ft and a flat leading edge. There are several reasons for choosing this shape. For example, it is a shape not easily adaptable to other methods of solution. Also, heat-transfer analyses have generally considered bodies with convex leading edges; therefore, most heat-transfer data are expressed in terms of nose radius which leaves one at a loss in predicting heat transfer rates to a flat-faced body.

The body was assumed to be at zero angle of attack and the gas was assumed to be not only gray and optically thin, but also thermally and calorically perfect. The only purpose of these assumptions was to reduce the computations.

Modified Lax Method

In the numerical calculations flow properties at a point in the computation net were found by averaging the properties of the four net points surrounding the point. Lax's method uses the properties of the surrounding points at the same time step. This method was modified by using the properties of the points at the current time step calculation; i.e., since the calculations were performed by a forward step in the positive x and y directions, the properties at the net point before and the point below were the properties at time $t+\Delta t$ while the properties of the point after and the point above were the properties at time t. This modification was found to strengthen the stability of the difference equations and also saved computer storage space.

Radiation

To include the effects of heat transfer by radiation in the

Received September 2, 1971; revision received December 23, 1971.
Index category: Radiatively Coupled Flows and Heat Transfer.
* Associate Professor of Aerospace Engineering. Member AIAA.